



A mesoscale modeling study of wind blown dust on the Mexico City Basin

Rafael Villasenor*, M.T. López-Villegas, S. Eidels-Dubovoi, Arturo Quintanar, J.C. Gallardo

Instituto Mexicano del Petroleo, Eje Central Lazaro Cardenas 152, 07730, Mexico DF

Received 14 October 2002; accepted 5 March 2003

Abstract

The latest phase of the program to improve the air quality in the Valley of Mexico, also known, as Pro Aire is about to go into effect for the next 10 years. Pro Aire puts emphasis on agricultural wind erosion and associated dust emissions impacting downwind air quality. The main objective of this investigation was to use an empirical USEPA erosion model coupled to a meteorological/transport-dispersion prediction model, CALMET/CALPUFF, to estimate dust emissions and concentrations in the Mexico City Basin. The model simulations for particulate matter (PM₁₀) are validated against observations taken at the most recent research field study, the IMADA–AVER field campaign, conducted during the spring of 1997 to provide information about high ozone, particulate matter concentrations and visibility impairment. The spatial and temporal PM distribution in the region is presented for a specific wind blown dust event consisting of two IMADA days, in order to understand how soil dust emissions from agricultural fallow land affect downwind areas during the dry season. Results show good agreement with the main spatial features of the local wind circulation and wind blown dust concentrations. A correlation coefficient of nearly 0.8 between predictions and observations for a modeled day suggests that an important portion of the total measured concentration had geological origin. This work constitutes an essential advancement on the mesoscale air quality problem on the MCMA due to wind erosion.

© 2003 Elsevier Science Ltd. All rights reserved.

Keywords: Windblown dust; Emission inventory; Mesoscale air quality modeling; PM₁₀ concentrations; Mexico City visibility reduction, wind erosion

1. Introduction

The Mexico City Metropolitan Area (MCMA) is one of the world's largest, polluted metropolitan areas, containing nearly 20 million inhabitants within the Mexico City Valley. Despite great efforts by the local and federal authorities to improve air quality, Mexico City's pollution levels continue to violate air quality standards. As in many large cities, and especially those located in valleys with high solar radiation, Mexico City

experiences severe air pollution episodes, particularly for ozone and suspended particles.

Three distinct major PM emission scenarios, occurring every year, involve different meteorological conditions. In wintertime automobile emissions, re-entrained road dust on paved city streets, and fugitive dust from unpaved roads and parking lots become significant sources. During early spring, in addition to the these urban PM emissions, the MCMA is prone to periodic wind erosion events, in which wind blown dust occurs from localized sources within the Mexico City basin. In summer and fall automobile emissions predominate as well as those from residential and industrial combustion sources. The only easing effect during the summer and

*Corresponding author. Av. Platanales 252-5 Col. Nueva Santa Maria, 02800 Col. Nueva Santa Maria, Mexico.
E-mail address: rvillase@imp.mx (R. Villasenor).

fall months can be observed by a wash-out of suspended particles due to more frequent rains than during the winter and spring months.

A comprehensive air quality study (<http://www.sbg.a-c.at/ipk/avstudio/pierofun/mexico/air.htm>; April, 2002) of the Mexico City airshed reports that the main sources of most pollutants are internal combustion engines (75%), followed by natural sources (12%), services (10%) and industries (3%). At thinner atmospheres fossil fuel combustion is far from ideal and the increased incidence of solar radiation when combined with primary pollutants accelerates the photochemistry that leads to higher ozone and aerosol concentrations. The massive generation of toxic gases on the high-altitude basin is responsible for a persistent visibility reduction in the MCMA. A further deterioration of the air quality conditions occurs during the dry season when wind energy, which is the driving force of both wind erosion and dust suspension, surpasses a threshold surface velocity. When surface winds are above the threshold velocity wind erosions takes place.

Mountainous terrain at subtropical latitude and high elevation surrounds the region where the MCMA lies. Situated at an average altitude of 2240 m above sea level, the average atmospheric pressure is roughly 25% lower than at sea level. The climate is predominantly semiarid owing to its elevated location. A recent study (Molina and Molina, 2000) shows that the daily standard for particulate matter 10 μm or less (PM_{10}) has been exceeded on numerous times since measurements were started in 1995, with several of this occasions occurring on days of obvious regional agricultural wind erosion. The current EPA standards for PM_{10} that the Mexican regulation use for air quality control is actually composed of both an acute (24 h allowable average) and chronic component (annual allowable average): A 24 h average not to exceed $150 \mu\text{g m}^{-3}$ of air more than three times in 3 years; and an annual arithmetic average not to exceed $50 \mu\text{g m}^{-3}$.

Land use within the area of Mexico City has been drastically modified in the last 30 years due to an explosive population growth, increased industrial activity, and reductions in green areas neighboring the city. The Federal District that encompasses 13 counties plus 16 counties of the State of Mexico forms the MCMA. The MCMA area is delimited by two mountain ranges to the southeast and southwest at the center of the topography map of the Mexico City Valley that Fig. 1 shows. Within these political boundaries of the MCMA all major socioeconomic activity takes place. The location of agricultural non-irrigated areas is found mainly to the northeast, which are usually fallow from February until May when rain is scarce. Fig. 1 shows the soil dust areas in dark, scattered throughout the MCMA. It is these large dusty areas that are susceptible to wind erosion events during the dry season. There are

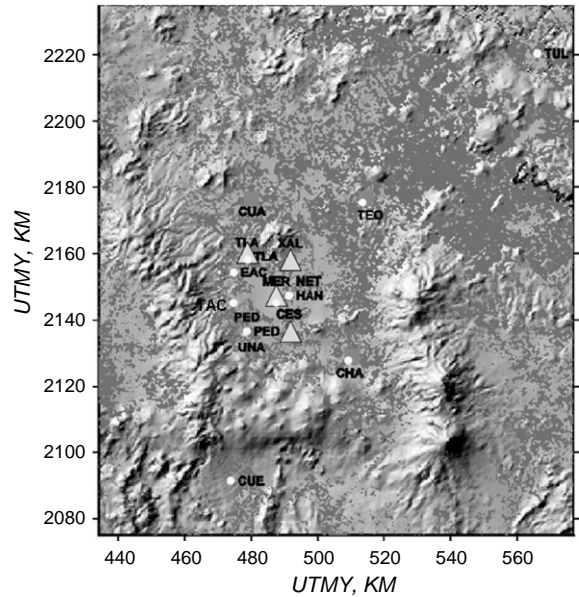


Fig. 1. Map of topography of the Mexico City Metropolitan Area showing fallow land (brown areas), air quality monitoring PM stations (triangle), surface meteorological stations (circle), upper air soundings locations (square).

significant terrain features along the southwest and southeast boundaries of the MCMA as depicted in the physical domain of Fig. 1. Between the two mountain ranges there is a mountain pass where topographically confined airflow is channeled into and outside the MCMA. The surrounding mountain ranges act as barriers to air pollutants restricting the horizontal ventilation, and allow the up slope and down slope flows to develop during the diurnal cycle.

A typical pattern that produces high PM_{10} concentrations in the Mexico Basin cannot be described by the typical conceptual description of most mid-latitude valleys and basins (Oke et al., 1993; Whiteman et al., 2000). Collins and Scott (1993) claim that air quality in the Mexico Basin is exacerbated by strong temperature inversions that form within the elevated basin. A more recent study of the boundary layer evolution and diurnal flow circulation over the Mexico Basin and Mexican plateau challenges this view (Whiteman et al., 2000). With data collected in an intense measurement campaign in February and March 1997 (IMADA, 1999; Fast et al., 1998) Whiteman and co-workers (Whiteman et al., 2000) noticed that the mean morning low-level stability was only marginally greater than in the free atmosphere surrounding the Mexican plateau at the same altitude. Therefore, the Mexico Basin does not appear to exhibit one of the chief meteorological characteristics of mid-latitude basins, namely the formation of strong nighttime temperature inversions.

A correct description of the meteorological processes is thus fundamental to predicting the three-dimensional distribution of PM in the region, and is necessary in order to understand how emissions from various sources affect visibility and aerosol formation.

The daily rhythm of the circulating airflow in the MCMA has been described elsewhere (Whiteman et al., 2000; Orea, 1999; Edgerton et al., 1999; Doran et al., 1998; Fast and Zhong, 1998). Briefly, the general characteristic of the wind pattern takes place in three stages. In early morning, synoptic flow has an impact on the local and regional thermally driven flows in the MCMA. The cool masses of air sink along the slopes of the mountain ranges sliding underneath the stagnant cold pollutant blanket of air covering the MCMA. As the sun heats up the basin, advection mechanisms vertically and horizontally gradually shift to create a convective cell as the cold air parcel rise with an increasing heat flux input. The synoptic flow of the upper troposphere sweeps out the masses of air that rise further in the late afternoon. The mixed layer extends beyond the peaks of the surrounding mountains, thus the basin is observed to remain reasonably well ventilated during the diurnal cycle. A direct consequence of capping entrainment of synoptic flows suggest that air pollution in the MCMA tends to be exacerbated by continuous emission of sources due to the socio-economic activity and daily operations in which large numbers of mobile, point and area sources are involved, since ventilation coefficients in the region are usually high in this complex topographic setting.

The Mexico basin periodically experiences wind blown dust events that cause exceedances of the national ambient air quality standard for PM₁₀. Blowing dust normally involves local entrainment of dust and each event is associated with moderate or large winds occurring in early spring when temperatures are high and humidity is low. Wind blown dust sources are agricultural lands that surround the periphery of the MCMA to the north and northeast sector of the basin. In the dry season, when the land becomes fallow, urban areas nearby are exposed to high PM concentration. A climatic summary of the airborne dust environment in the region reveals that the intensity and frequency of dust events downwind of geological sources takes place in the month of March (Mexican Air Space Navigation Service, 1999). The frequency of wind blown dust events was compiled from a 10-year climatic database spanning from 1988 to 1998. Concurrently, an analysis of the IMADA-AVER (Investigación sobre Materia Particulada y Deterioro Atmosférico—Atmospheric Aerosol and Visibility Research) database (IMADA, 1999) taken during the month of March in 1997 using chemical concentrations of five crustal species (Al, Si, Fe, Mg, K and Ca) shows (Edgerton et al., 1999) that geological material was the major contributor to PM₁₀. In fact,

40–55% of the PM₁₀ mass was of geological origin at two sites downwind of soil eroded areas. This implies that deposition mass fluxes at local urban sites near potential soil sources are quite significant when compared to the rest of the sources in the MCMA.

Particulate matter was considered in the 1989 emission inventory (EI) as total suspended particles (TSP), and an updated version produced in 1994. Particle emissions were attributed mainly to soil erosion encompassing approximately 95% of the total particle inventory (Ruiz and Gasca, 2001). In the 1994-EI, particle emissions from sources other than erosion were considered for the first time. Primary PM₁₀ emissions from the most important sources, including the industrial sector, were considered in the 1996 EI. The 1998-EI, which includes economic activity data, is presented in the Federal District Government web page (Gobierno del Distrito Federal, 2001) with a soil erosion apportionment of 40%. This last inventory does not report emission estimates for TSP, but contains estimates for primary sources of PM₁₀ and PM_{2.5}. Differences in methodology and changes in activity data among the 1994, 1996 and 1998 emissions inventories have made it difficult to correlate emissions figures with pollution control strategies in the MCMA. Even though the latest version of the EI has undergone several updates in the last decade (Instituto Nacional de Ecología, 2001) the number of uncertainties is still substantial. Therefore it becomes necessary to have other means to better estimate the apportionment of dust emission to the total EI for PM.

The latest phase of the program to improve the air quality in the Valley of Mexico, also known as Pro Aire (Gobierno del Distrito Federal, 2001), is about to go into effect for the next 10 years. The program puts emphasis on agricultural wind erosion and associated dust emissions impacting downwind air quality. There is an increased need for a prediction method to estimate dust emissions and concentrations on a wind event basis before this program is fully implemented. A project to characterize PM sources and to model PM at a regional scale in the MCMA was carried out at Instituto Mexicano del Petroleo (IMP) in order to develop an empirical method to estimate dust emissions in this region. The complete database taken during the IMADA campaign of March 1997 provided the much-needed observations for model verification in efforts to study relationships between PM₁₀ particulate pollution and agricultural field wind erosion. With model predictions, the PM contribution due to wind erosion to the EI in the MCMA can be better estimated.

Previous air quality studies on the MCMA focused on the origin of high concentrations of particles including the spatial and temporal distribution of some gaseous pollutants (Doran et al., 1998; Fast and Zhong, 1998). Some drawbacks to those studies should be noted. First,

the domain of study excluded the regions that are prone to soil erosion since the inner grid was $120 \times 120 \text{ km}^2$ in size. Second, by using a Lagrangian approach (Fast and Zhong, 1998) particles were randomly released without associating them to any particular PM sources in the MCMA, despite that, each particle was tagged by its release location, release time, and current position so that the history of a particle plume and individual trajectories could be obtained. This was done to examine the meteorological patterns in the valley. A recent work (Edgerton et al., 1999), however, finds that the highest observed PM concentrations occur on the northern and eastern parts of the Mexico City Valley, in contrast to the high ozone concentrations normally found towards the southwest.

2. Air quality field study

The ambient monitoring component of IMADA–AVER took place over a 4-week period from 23 February to 22 March 1997 (IMADA, 1999). Of the 28 days monitored with particle samplers, samples taken from 2 to 19 March 1997 (18 days) were analyzed for elements, ions, and elemental and organic carbon. This period contains three distinct episodes of pollution buildup and cleanout. The period before 8 March was relatively dry, while the subsequent episodes occurred during moist weather conditions, interspersed with fogs, clouds, and rainstorms. Meteorological data included radar wind profiles, remote acoustic sounding system (RASS) temperature sensors, and temperature and humidity profiles by airsonde and surface meteorological towers (Gobierno del Distrito Federal, 2001). For

particle measurements the following air quality monitoring stations within the MCMA were used: Xalostoc (XAL), Merced (MER), Cerro de la Estrella (CES), Pedregal (PED), Netzahualcoyotl (NET) and Tlalnepantla (TLA). Samples from the first three sites were collected every 6 h and for the last 3 every 24 h. From these particle measurements the total PM_{10} and $\text{PM}_{2.5}$ concentrations as well as their geological origin were determined (Watson and Chow, 1998; Vega et al., 2001). The IMADA study also included measurements of light absorption and scattering by particles with an aethalometer and a nephelometer (Silvia, 2002) at a commercial (MER) and residential sites (PED).

3. Modeling episodes

Several parameters were examined in order to select the wind erosion episode for air quality simulations. Among these parameters is visibility (Vis), which is an important air quality variable related to the coefficient of visible light extinction (bext) through Koschmieder relationship $\text{Vis} = 3.912/\text{bext}$. Extinction of light, in the atmosphere is due to absorption and scattering of light by gases and particles. The gaseous contributions to light extinction in the visible region are generally small and limited to absorption by NO_2 and scattering by molecular oxygen and nitrogen (Rayleigh scattering). On the other hand, particles in the size range $0.1\text{--}1 \mu\text{m}$ either emitted directly or formed via photochemical mechanisms are the main contributors to visible light extinction. In the visible, particle absorption is only due to elemental carbon (EC), whereas a wide range of aerosol compositions produces particle scattering.

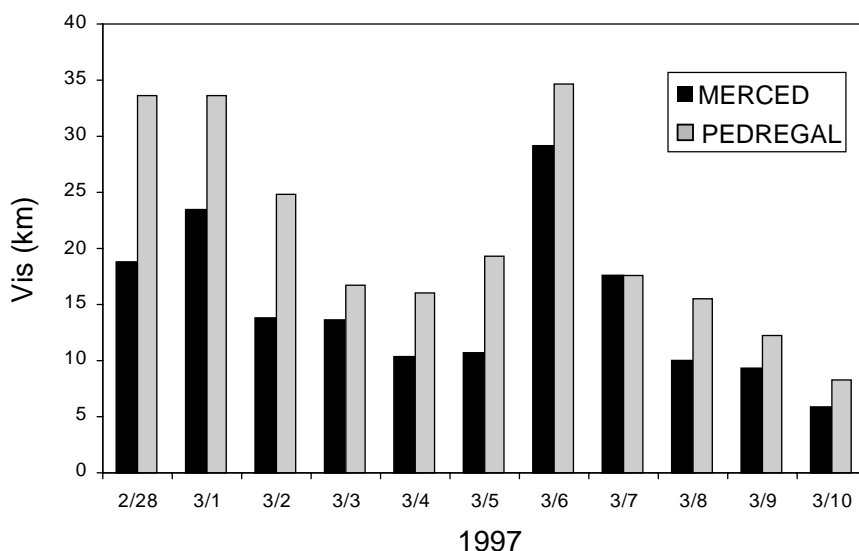


Fig. 2. Daily average visibility from 28 February to 10 March 1997 at the MED and PED air quality-monitoring sites.

Fig. 2 shows the calculated daily average visibility for 11 days, 28 February–10 March 1997 selected from the IMADA measurement period. In this calculation, the contribution to light extinction of both particles and gases was taken into account, albeit the minor contribution of gases. Since the main contributor to total light extinction is light scattering by particles, it is likely that photochemical processes dominated those days in which visibility was very poor. However, visibility impairment also occurs because of the presence of primary pollutants. In the MCMA when strong surface winds converge into the valley and their influence is felt on the basin's dusty areas, such as fallow land, visibility is reduced. Soil dust emissions from agricultural areas and paved and unpaved roads tend to reduce visibility if the wind energy is enough to surpass a threshold wind velocity characteristic of the soil type.

Two important scenarios of very poor air quality conditions are evident in Fig. 2. One of them took place on 4 and 5 March. The obvious visibility improvement on 6 March indicates that the concentrations of particles in the size range 0.1–1 μm significantly dropped at both the MER and PED sites. The second scenario, which is actually longer, starts on 7 March. Systematically, visibility decreases attaining its lowest value on 10 March, the last day of the period selected for visibility analysis. The analysis of the PM_{10} concentrations recorded at several air quality monitoring stations and the meteorology of the period indicate that a wind blown dust event occurred on 4 and 5 March while photochemical mechanisms dominated on 7–10 March.

Surface meteorological measurements showed that strong winds had begun after mid-day on 5 March and continued on through for the most part of 6 March. The vertical profiles of the wind flow structure also indicated that synoptic winds had swept across the Mexico City Valley exerting their influence near the earth surface, hence removing pollutants from the valley. Clear skies dominated on 6 March with a nearly constant ambient air temperature of 15°C so that not only were the snow-capped volcanoes (Popocatepetl and Ixtacihuatl) to the east of the MCMA visible, but also the air was more breathable. Haziness due to particles in the size range 0.1–1 μm was at its lowest level on 6 March, as Fig. 2 shows. On 5 March the highest PM concentrations were observed dropping to practically negligible values in the later parts of the day, attaining a significantly low value throughout 6 March when compared to national ambient air quality standards. Therefore the first scenario is indicative that a wind blown dust event had taken place on 5 March.

The second scenario, specifically from 7 to 10 March, appeared to be a pollution episode that was mainly driven by photochemical processes. Ozone observations from the automated monitoring network (RAMA) were used to discern the possible sources of PM. Under the premise that photochemical conditions dominated if O_3

concentrations were high it is hypothesized that significant PM was potentially secondary in nature from anthropogenic sources. If O_3 concentrations were low and significant PM concentrations occurred then PM concentrations were probably from primary emission sources, such as wind blown dust, especially if the wind was strong from the North and NE where the fallow agricultural fields lay. The hourly surface ozone concentrations for 5–10 March are presented in Fig. 3a. The contrasts in the peak ozone values are very distinct for 5 and 10 March, and as seen in Fig. 3a for the PED site a 70% increase in troposphere ozone was recorded.

The diurnal variability of EC, a primary emission from combustion sources, obtained from aethalometer measurements on 5, 6, and 10 March at the commercial site, MER is shown in Fig. 3b. This figure displays three important features. First, the profile for EC on 5 March during the first half of the day is significantly higher than on 10 March, which indicates that anthropogenic activity was higher on 5 March than on 10 March. 10 March however, was the day of lowest visibility. Second, the EC profile from the afternoon of 5–6 March is flat and nearly constant as the synoptic winds swept the valley. Third, the EC profile does not undergo drastic diurnal changes for 10 March. It remains fairly constant except for a sudden increase at 1800 h.

A comparison of the geological contribution to PM_{10} between these two scenarios helps to further clarify the events of 5, 6 and 10 March. At PED the five crustal-species contribution to PM_{10} measured 29%, 31% and 19% for 5, 6, and 10 March, respectively. The percentage at MER for the days given in the same order as above are slightly different but preserve the same trend; 36%, 35%, 18%. From these percentages one sees substantial fossil fuel combustion activity on 10 March relative to geological dust emissions. Fig. 4, which depicts the $\text{PM}_{2.5}$ – PM_{10} ratio at both measuring stations for the three selected days in March further supports this fact, since the highest $\text{PM}_{2.5}$ fraction (approximately 60%) shows up on 10 March at either station.

Although the 24-h average concentration standard of 150 $\mu\text{g m}^{-3}$ was violated at four stations on 4 March (PED = 231 $\mu\text{g m}^{-3}$, MER = 200 $\mu\text{g m}^{-3}$, XAL = 170 $\mu\text{g m}^{-3}$, TLA = 168 $\mu\text{g m}^{-3}$), the wind energy that causes wind erosion was below a threshold surface wind speed. The meteorological conditions for that day were not as significant as with 5 March, in which four PM exceedances were also recorded: PED (210 $\mu\text{g m}^{-3}$), MER (246 $\mu\text{g m}^{-3}$), TLA (235 $\mu\text{g m}^{-3}$), and CES (231 $\mu\text{g m}^{-3}$), and none were recorded on 10 March. Surface stations on 5 March recorded maximum temperature and relative humidity as 28°C and 50%, while on 6 March they were at 18°C and 80%. The average surface wind speed for these three days at the MER and PED sites is as follows. For 10 March the calculated 24-h average surface wind speed was

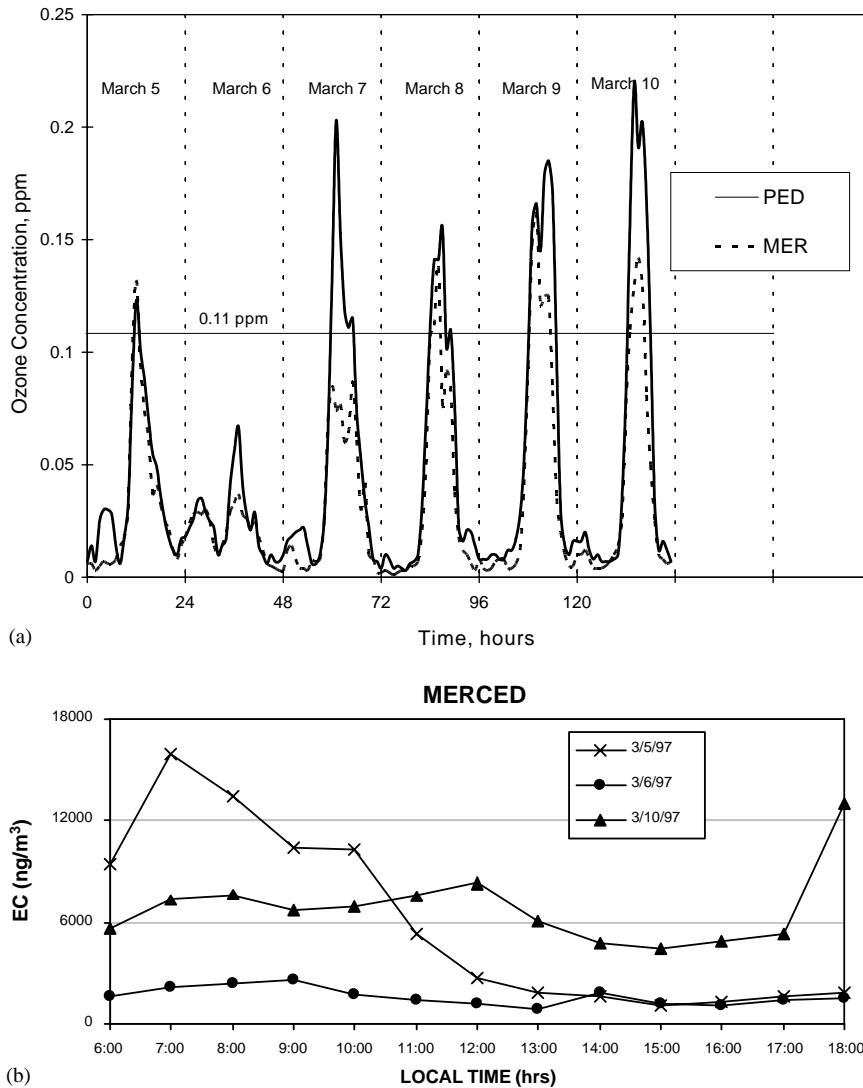


Fig. 3. (a) Hourly surface ozone concentration for 5–10 March 1997 at the MER and PED air quality-monitoring sites, showing the 110 ppb hourly ozone standard as the horizontal line. (b) Hourly elemental carbon concentration for 5, 6 and 10 March 1997 at the MER air-quality monitoring site.

1.3 m s^{-1} , whereas the magnitude of the computed surface wind speeds for 5 and 6 March came as 2.8 and 3.2 m s^{-1} , respectively. It must be noted that 5 and 6 March have not been considered in past studies of transport and dispersion of pollutants due to the fact that attention was focused on the meteorology and transport of gaseous pollutants within the MCMA. Also these days were examined by other authors to be atypical in the sense that synoptic conditions led to unusually strong wind within the MCMA (Whiteman et al., 2000). Despite significant anthropogenic activity on 5 March, as indicated by the EC measurements, wind blown dust was the major contributor to elevated PM_{10} concentrations on this day. The parameters that played

a major role to define the wind blown dust event were the wind speeds, drier/hotter conditions, lower $\text{PM}_{2.5}/\text{PM}_{10}$ ratios and higher geologic/ PM_{10} ratios. Therefore, in this study, 5 and 6 March 1997 were chosen for modeling simulation to estimate wind erosion and dust emission owing to the obvious manifestation of contrasting meteorological features and distinct air quality conditions concerning a typical wind blown dust event.

4. Wind erosion model

Emissions from rural areas are a concern in the Mexico City Basin because of the existence of

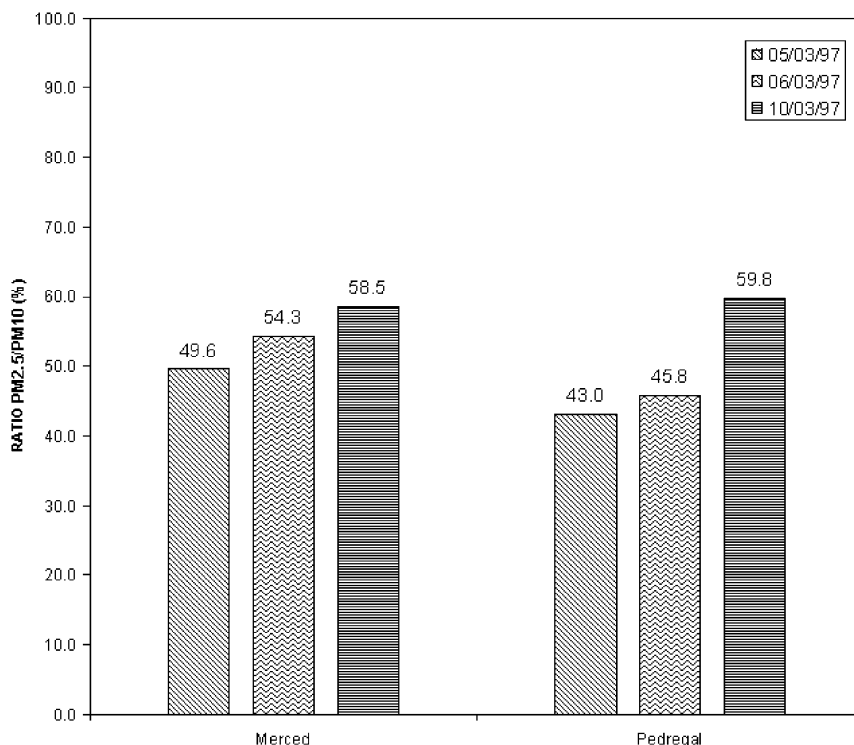


Fig. 4. Ratio of $PM_{2.5}$ - PM_{10} at the MER and PED air quality-monitoring sites for 5, 6 and 10 March 1997.

agricultural fields and uncultivated soil with minimum or no vegetation coverage. Wind blown dust from sources on the north and northeast areas outside of the urban area invariably intensify in the month of March and the impact of soil dust emissions and concentrations have never been predicted through the use of mathematical modeling. In this work a wind erosion equation approach has been applied to generate the necessary input to a transport-dispersion simulator for a selected event that caused regional particulate concentrations to exceed $150 \mu\text{g m}^{-3}$ ambient standard. The algorithm that predicted dust concentrations was developed from data taken from wind tunnels and field studies to produce a wind-erosion-prediction equation ([Wind Erosion Research Unit](#)). The Natural Resources Conservation Service (NRCS) has used the wind erosion equation. It is a popular method for assessing average annual soil loss by wind from agricultural fields. There is a more recent PM_{10} dust flux model published in the literature ([Saxton, 1995](#)) that was developed from extensive field data throughout the Colombia Plateau of Eastern Washington State. Model results have shown quite reasonable agreement with downwind dust concentrations for several historic events ([Claiborn et al., 1998](#)). This model has the capacity to estimate dust emissions from a variety of regional situations but lack of field measurements in the MCMA impedes its application at

this time. Details on the wind erosion equation and the parameters that were used to apply this equation for the MCMA soil sources can be found elsewhere ([Gobierno del Distrito Federal, 2001](#)).

5. Domain and modeling approach

The CALMET/CALPUFF modeling system was selected to model the meteorology and pollutant transport of a wind blown dust event in the MCMA. CALPUFF has been traditionally used in US. Environmental Protection Agency's (EPA) regulatory applications, where environmental impacts due to routine industrial releases or wild fires are modeled. The errors associated with the loss of pollutant mass at the edges of the computational grid boundary were recently evaluated for CALPUFF considering different modeling domain sizes ([Venegas et al., 2002](#)). The average percent error increased with additional volume sources and as the computational domain size approached a $100 \text{ km} \times 60 \text{ km}$ grid mesh. In this work only the emissions sources due to wind erosion have been considered and the size of the domain was chosen to be 3.7 times higher than the size of the domain mentioned in reference ([Venegas et al., 2002](#)). Three main components comprise this modeling system:

CALMET (Scire et al., 1997) (a diagnostic three-dimensional meteorological model), CALPUFF (Scire et al., 2000) (the transport and dispersion model), and CALPOST (a postprocessing package). Each of these programs has a graphical user interface (GUI). In addition to these components, there are several other processors that may be used to prepare geophysical (land use and terrain) data in many standard formats, meteorological data (surface, upper air, precipitation, and buoy data), and interfaces to other models such as the Penn State/NCAR Mesoscale Model (MM5) (Dudhia et al., 1994). In the present study only surface meteorological observations and upper air soundings were used to drive CALMET.

5.1. The diagnostic meteorological model, CALMET

The first component of this system, CALMET, is a diagnostic wind field generator (Scire et al., 1997) that uses surface and upper air meteorological data to compute winds and turbulence parameters in each grid of the modeling domain for each hour of a modeling period. CALMET is a mass-conserving meteorological model initialized with hourly meteorological data from the observational IMADA–AVER network and land-use data. The model can be considered in this sense as a physical space and time interpolator since it includes a number of physical processes that account for atmospheric–surface interactions such as topographic effects and turbulent processes for the atmospheric boundary layer. Another correction includes an energy balance calculation, which takes into account the radiation balance at the surface and the presence of clouds. The model is “nudged” to the observational data with the mass conservation constraint before the final corrected wind field is produced.

Surface and upper air soundings were used to compute the interpolated wind field. Eleven meteorological surface stations are deployed throughout the MCMA. The UTM coordinates of these stations (MER, CHA, TAC, TEO, UNAM, TUL, EAC, TLA, PED, CUE and HAN) are given in Table 1. The upper air soundings were released at four sites (CHA, CUA, UNAM, and TEO) with coordinates also given in Table 1. The origin (southwest corner) of the computational domain in UTM coordinates was placed at (434,2080) km.

It was assumed that a 5-km horizontal resolution was reasonably accurate for model resolution, while allowing for an acceptable execution time. The grid system extends to the north and east creating a uniform grid system of horizontal squares of surface area equal to 25 km². CALMET performed 24-h simulations on two consecutive days for the 14 UTM zone. The maximum radius of influence over land in both the surface layer and aloft was taken as 5 km with a maximum acceptable

Table 1

UTM coordinates of the meteorological surface stations and upper-air sounding sites that CALMET used for the Mexico City metropolitan area simulations

Surface meteorological stations	UTM _x	UTM _y
Merced (MER)	487.5	2147.5
Chalco (CHA)	509.5	2128.4
Tacubaya (TAC)	479.1	2145.1
Teotihuacan (TEO)	515.7	2176.1
UNAM	480.3	2136.2
Tulancingo (TUL)	566.3	2220.5
ENEP Acatlan (EAC)	474.6	2154.5
Tlanepantla (TLA)	478.5	2159.3
Hangares (HAN)	491.3	2147.5
Pedregal (PED)	478.6	2136.7
Cuernavaca (CUE)	477.9	2090.3
Upper air soundings		
Chalco (CHA)	509.5	2128.4
Cuautitlan (CUA)	480.1	2177.1
UNAM	480.3	2136.2
Teotihuacan (TEO)	515.7	2176.1

divergence in the divergence minimization procedure of 5.0×10^{-6} . The complex topography of the MCMA considers 13 land use categories. The CALPUFF model uses the same grid system as CALMET, consisting of 9 layers over the 28×32 horizontal grid cells. The vertical layers were specified with variable spacing at heights of 20, 80, 160, 300, 600, 1000, 1500, 2000, and 2130 m.

5.2. The air quality model CALPUFF

Once the diagnosed three-dimensional wind field and micro-meteorological variables are generated and the area source emission of soil dust inventoried, these are input into the next component of the modeling system, CALPUFF. The transport and dispersion model, CALPUFF, advects “puffs” of PM emitted from modeled sources, simulating the dispersion and transformation process at each grid cell. In our case the pollutant has been assumed to behave as a passive scalar and hence no chemical transformation takes place. The primary output files from the non-steady-state Lagrangian Gaussian puff model contain hourly concentrations at all receptor locations but only MER, CES, and XAL were used for comparison since these are closer to the soil dust sources.

All potential dust sources are considered to fall inside a domain that extends 140 km in the eastward coordinate and 160 km in the northward coordinate. Other classes of PM sources such as from paved roads, unpaved roads and unpaved parking lots are not considered in this study. The vertical concentration distribution in the near field is considered to be

Gaussian. Dispersion coefficients are computed from internally calculated velocity variances using micrometeorological variables supplied by CALMET. CALPUFF models dry deposition and the emitted PM₁₀ species are modeled assuming they behave as particles. The mean and standard deviation are used to compute a deposition velocity for size-ranges, and these are then averaged to obtain a mean deposition velocity. Some miscellaneous dry deposition parameters include the reference cuticle resistance, 30.0 s cm^{-1} , and the reference ground resistance, 10.0 s cm^{-1} . The area sources (tons/m²/year) were taken as a composite of irregular polygon surfaces that match soil eroded maps obtained with a satellite imaging technique (Orea, 1999). The total surface area susceptible of erosion is approximately 1200 km², which is comparable in size to that of the MCMA. The geophysical parameters that define the soil dust properties were taken as default values as given in reference (Wind Erosion Research Unit).

6. Model results

This section describes the 48-h air quality simulations for 5 and 6 March using the CALMET/CALPUFF modeling system. Contour maps of surface wind speed, mixed layer heights and predicted PM concentrations are discussed in the following paragraphs.

Fig. 5 shows two panels for 5 March at 06:00 h as simulated by CALMET and CALPUFF. Fig. 5a shows the surface wind vectors and surface temperature contours while Fig. 5b presents mixed layer depths and wind blown dust concentration. Computations at this hour of the day are similar in shape and intensity to the earlier hours of simulation. At 06:00 h light-to-moderate easterly winds blow over the two major dust sources located northeast of the MCMA causing entrainment and suspension of dust. Over the eastern mountain range, cool air descends with an easterly component, leading to air streams that cause minor convergence at the center of the MCMA. Two scenarios are observed in Fig. 5 in regard to the soil sources. Winds with a northerly component advect dust plumes into the MCMA basin where downslope flows from the western mountains then advect the dust plumes eastward causing higher concentrations along the slopes of the eastern mountains. Thus, lower PM concentrations occurred at the PED and MER sites (in the southwestern region of the basin), as predicted by CALPUFF. The mixing layer height remains relatively shallow over the domain of interest for much of the morning period, but PM concentrations tend to remain relatively high near the erosion sources. The western portion of the MCMA remains unaffected by wind blown dust partly due to westerly winds that counteract the effect of the spreading dust cloud.

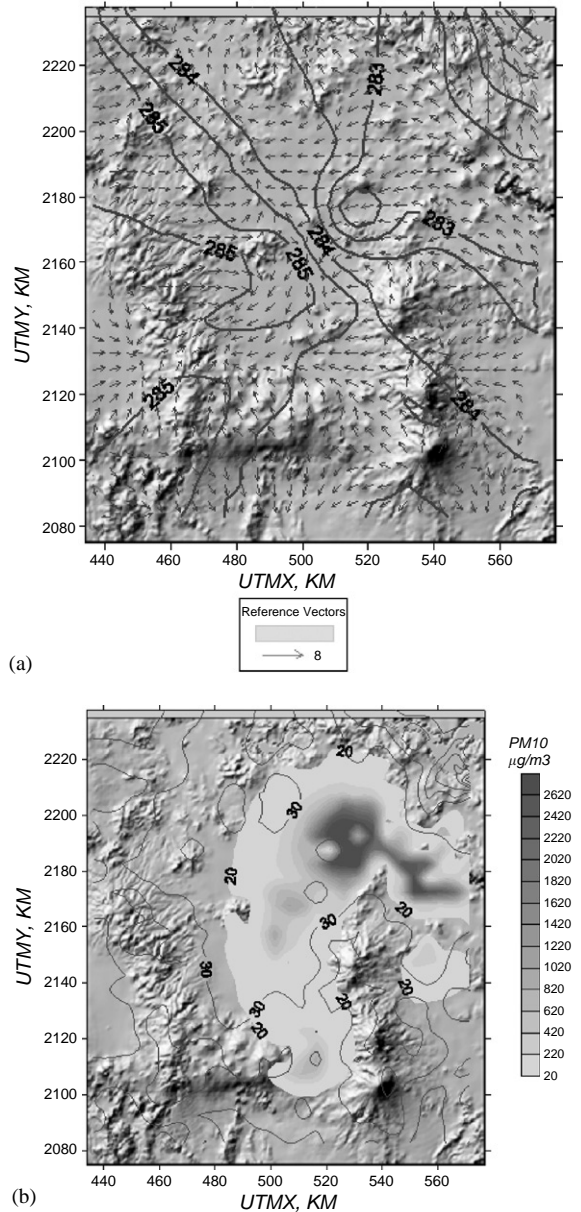


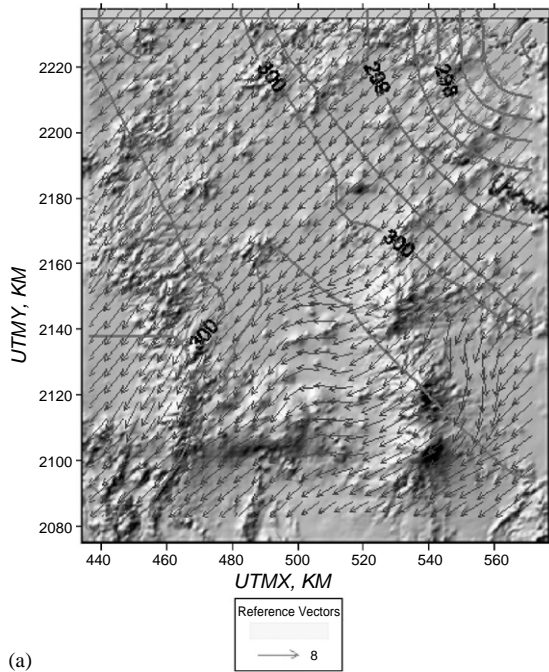
Fig. 5. (a) Surface winds and surface ambient temperature contours for 5 March at 0600 h (b) mixed layer depth contours and dust concentration for 5 March at 0600 h.

The predictions at 14:00 h represents a transitional period characterized by low concentration of particulate matter measured at all the monitoring locations within the MCMA from 10:00 to 15:00 h (not shown). A significant increase in mixed layer heights over the MCMA going from 500 to 2000 m in less than 5 h highlights this period. In addition, the wind field displays large wind speeds (about 7 m/s) relative to the early hours with a northeasterly component throughout much of the MCMA. This is in accord with the lower

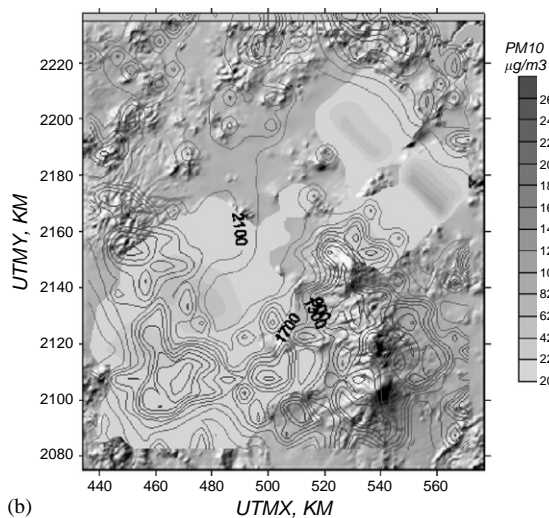
PM concentrations measured (not shown) during this time over the MCMA particularly at the industrial and urban areas. Fig. 6 shows similar vector and scalar fields as Fig. 5 except shown at hour 18:00. The winds have a well-defined northeasterly component all over the physical domain and they are responsible for transporting measurable amounts of geological dust to the densely populated areas of the MCMA. This constitutes the second most important concentration peak of

5 March; during this hour PM concentrations over the southern part of the MCMA attained a second maximum before they slowly decayed in the late evening hours.

The diurnal evolution of predicted PM concentrations of geological origin for 6 March show (not shown) a similar spatial behavior as those found during the simulation of 5 March but with significantly lower values. The key feature to note here is that from 5 to 6 March a strong northerly basin-to-valley wind was driven by a cold and humid air mass as evidenced from a large temperature drop to the north of the MCMA in the evening of 5 March. This cold air mass pushed its way through the basin and helped maintained the strong northerly wind blowing through most of 6 March, thus resulting in a cleaner airshed and a better visibility. Fig. 7 shows the scatter diagrams of predicted wind blown dust concentrations (C_p) versus the observed ones (C_o) for 5 and 6 March for the XAL, NET and MER stations. On 5 March the predicted concentrations show a much better correlation to the geological component of measured PM concentrations when compared to 6 March. The significant agreement between predictions and observations for 5 March suggest that much of the suspended PM in the airshed came from sources associated to agricultural fields located on the northeast sector of the MCMA. By contrast, the poor agreement between predictions and observations for 6 March suggests that the PM concentrations measured at the receptor sites had a more significant contribution from local geological sources than the drier dust of agricultural areas. The disagreement between observations and predictions for 6 March are likely due to omissions of other potential PM sources such as paved and unpaved roads that were not accounted for in the EI.



(a)



(b)

Fig. 6. (a) Surface winds and surface ambient temperature contours for 5 March at 1800 h (b) mixed layer depth contours and dust concentration for 5 March at 1800 h.

7. Conclusions

Two contrasting air quality scenarios were identified from 4 to 10 March of the IMADA field study, a wind blown dust event and a photochemical event. The analysis of the visibility trend and of the EC profile resulting from IMADA data in conjunction with hourly ozone and PM_{10} concentrations obtained from the RAMA ambient network aided in the identification of these scenarios. Hourly PM_{10} concentrations measured at RAMA showed violations of the PM standard on 4 and 5 March with unusually higher concentrations on 5 March, and none on 10 March. The calculated $PM_{2.5}$ – PM_{10} ratio using IMADA data at two receptor sites supported the hypothesis of a wind blown dust event. The main driver of wind erosion on agricultural fallow land was the effect of strong synoptic winds that started at mid-day on 5 March

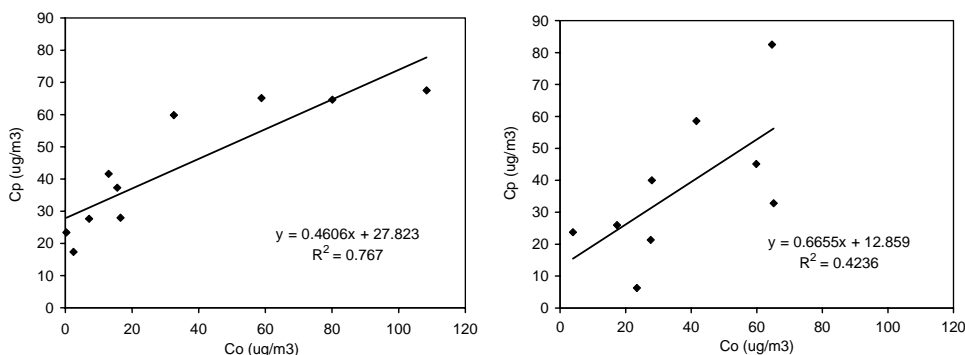


Fig. 7. Scattered plots of predicted vs. observed PM concentrations for 5 March (left panel) and 6 March (right panel) 1997 for the XAL, NET and MER stations.

and continued on until the later hours of 6 March. The low visibility of 10 March, together with the high surface ozone levels, was solely attributed to anthropogenic activity in which the concentration of particles in the size range 0.1–1 μm significantly increased at both the MER and PED sites. The days of 5 and 6 March 1997 were chosen for air quality model simulation as typical candidates for a wind blown dust emissions on a wind event basis.

The simulation of the spatial and temporal evolution of PM concentrations predicted with the CALMET/CALPUFF modeling system showed reasonable agreement with the observed particle measurements of geological origin for 5 March. A correlation coefficient of nearly 0.8 gives enough confidence to suggest that an important portion of the total measured concentration had geological origin. The poorer correlation between model predictions and observations for 6 March indicates that the PM concentrations measured at the MER and PED sites were from other dust sources within the vicinity of the receptors.

The prediction method that was adopted for the Mexico basin is the first of its kind to be used for estimating dust emissions and concentrations on a wind event basis. One of the benefits of the dust emissions simulations is to use it for reducing the level of uncertainties that are inherent in the measurement data at individual sites. This may be so as some of the receptors may not be representative over larger areas due to the complexity of the terrain; and because of the lack of horizontal resolution of the IMADA and RAMA air quality networks. The CALMET/CALPUFF modeling work complemented the observations data by allowing our research group to gain further insight into the wind blown mechanism at the MCMA that sets in at the onset of increasingly stronger synoptic winds in the dry season.

A shortcoming of the wind erosion approach used in this work was the procedure that calculates the PM_{10} dust fluxes, which were based on a composite of

irregular polygon surfaces that match soil eroded maps obtained with a satellite imaging technique. The PM_{10} vertical fluxes need to be measured on site to reduce uncertainties in the simulations, and to have a more accurate representation of the phenomenon of wind erosion in the MCMA.

Although this work constitutes an essential advancement on the regional air quality problem on the MCMA due to wind erosion, more work is still needed in this undeveloped area. A more realistic emission algorithm, such as the one developed by Saxton (1995) for PM_{10} dust will provide better estimates of mass concentrations when simulating historic and recent events. This task requires field measurements of soil dust parameters, including threshold velocity, erodibility rank, and dustiness index. Land use parameters, including soil cover, surface roughness, water content and aerodynamic surface roughness for the MCMA should also be considered in the wind erosion algorithm. The high level of detail of the Saxton prediction model demands that a full three-dimensional air quality model, such as CALGRID (Yamartino et al., 1992), be employed. CALGRID can track individually particulate matter from all major source categories, including paved road, unpaved roads, combustion sources, mobile sources, and wind erosion. This approach would demand the compilation of an extensive EI needed to drive CALGRID, in addition to the meteorological wind and temperature fields.

References

- Claiborn, C., Lamb, B., Miller, A., Beseda, J., Clode, B., Vaughan, J., Kang, L., Newvine, C., 1998. Regional measurements and modeling of windblown agricultural dust: The Columbia plateau PM_{10} program. *Journal of Geophysical Research* 103 (D16), 19753–19767.
- Collins, C.O., Scott, S.L., 1993. Air pollution in the Valley of Mexico. *Geography Review* 83, 119–133.

- Doran, J.C., Coulter, R.L., King, C.W., Lee, J.T., Sosa, G., 1998. Wind patterns affecting pollutant transport in Mexico City. 10th Conference on Air Pollution Methods. American Meteorological Society, pp. 333–337.
- Dudhia, J., Grell, G.A., Stauffer, D.R., 1994. A description of the fifth-generation Penn State/NCAR Mesoscale Model (MM5). NCAR Technical Note NCAR/TN-398+STR.
- Edgerton, S.A., et al., 1999. Particulate air pollution in Mexico City: a collaborative research project. *Journal of Air and Waste Management Association* 49, 1221–1229.
- Fast, J.D., Zhong, S., 1998. Meteorological factors associated with inhomogeneous ozone concentrations within the Mexico City Basin. *Journal of Geophysical Research* 103 (18), 918–927.
- Fast, J.D., Zhong, S., Doran, J.C., 1998. Meteorological and dispersion modeling studies during the 1997 IMADA–AVER field experiment. Spring Meeting of the American Geophysical Union, Boston, MA.
- Gobierno del Distrito Federal, 2001. *Inventario de Cd. Mexico*, 1998. <http://www.sma.df.gob.mx/publicaciones/aire/inventario1998>.
- IMADA, 1999. Instituto Mexicano del Petróleo, Investigación sobre material particulado y deterioro atmosférico. Informe Técnico.
- Instituto Nacional de Ecología (INE), 2001. Sistema Nacional de Información Ambiental, Calidad del Aire. http://www.ine.gob.mx/dggia/cal_aire/espanol/pubinv.html.
- Mexican Air Space Navigation Service, 1999. <http://www.sct.gob.mx>.
- Molina, M.J., Molina, L.T., 2000. Integrated Strategy for Air Quality Management in the MCMA, Report 7. MIT, Cambridge, MA.
- Oke, T.R., Spronken-Smith, R.A., Jauregui, E., Grimmond, C.S.B., 1993. The energy balance of central Mexico City during the dry season. *Atmospheric Environment* 33, 3919–3930.
- Orea, C.M., 1999. Caracterización ambiental de las áreas de emisión edafólicas de PM₁₀ en la zona metropolitana de la ciudad de México. MS Thesis, *CIEMAD*, IPN.
- Ruiz, M.E., Gasca, J., 2001. Urban Air Pollution and Forests: Resources at Risk in the Mexico City Air Basin. Springer-Verlag Ecological Studies Series, Springer, Berlin (Chapter 7).
- Saxton, K.E., 1995. Fugitive dust from agricultural wind erosion—a comprehensive research program, in particulate matter: Health and Regulatory Issues, VIP 49. Proceedings of an International Specialty Conference, Air and Waste Management Association, Pittsburgh, PA.
- Scire, J.S., Robe, F.R., Fernau, M.E., Insley, E.M., Yamartino, R.J., 1997. A User's Guide for the CALMET Meteorological Model (Version 5.0). Earth Tech. Inc., Concord, MA.
- Scire, J.S., Strimaitis, D.G., Yamartino, R.J., 2000. A User's Guide for the CALPUFF Dispersion Model (Version 5.0). Earth Tech. Inc., Concord, MA.
- Silvia, E.-D., 2002. Aerosol impacts on visible light extinction in the atmosphere of Mexico City. *The Science of the Total Environment* 287 (3), 213–220.
- Vega, E., Mugica, V., Reyes, E., Sanchez, G., Chow, J.C., Watson, J.G., 2001. Chemical composition of fugitive dust emitters in Mexico City. *Atmospheric Environment* 35, 4033–4039.
- Venegas, L., Hannaway, G.R., Poor, N.D., 2002. An evaluation of the errors associated with loss of puffs at the boundary of the CALPUFF modeling domain. Proceedings of the Air and Waste Management Association, Baltimore, June 23–27.
- Watson, J.G., Chow, J.C., 1998. Investigación sobre Materia Particulada y Deterioro Atmosférico-Aerosol and Visibility Evaluation Research. 1997 Annual Report, Prepared for US Department of Energy, Office of Health and Environmental Research, Germantown, MD.
- Whiteman, C.D., Zhong, S., Bian, X., Fast, J.D., Doran, J.C., 2000. Boundary layer evolution and regional-scale diurnal circulations over the Mexico Basin and Mexican Plateau. *Journal of Geophysical Research* 105 (D8), 10081–10102.
- Wind Erosion Research Unit, Wind Erosion Simulation models, <http://www.weru.ksu.edu/weps.html>.
- Yamartino, R.J., Scire, J., Carmichael, G., Chang, Y., 1992. The CALGRID mesoscale photochemical grid model-I model formulation. *Atmospheric Environment* 26a (8), 1493–1512.